Visualizing Temporal Behavior in Multifield Particle Simulations

T. S. Reis Santos[1], F. V. Paulovich[1], V. Molchanov[2], L. Linsen[2] and M. C. F. de Oliveira[1]
[1]*Instituto de Ciências Matemáticas e de Computacão, University of São Paulo, São Carlos, Brazil*
[2]*School of Engineering and Science, Jacobs University, Bremen, Germany*

Keywords: Volume-based Particle Visualization, Time-varying Visualization, Multidimensional Projection.

Abstract: Particle-based simulations generate time-varying multifield volumetric datasets. Visualizations of such volumes traditionally focus on the physical space, displaying particles as glyphs or with volume rendering techniques. In this paper we deal specifically with the issue of helping users to observe and interpret the multidimensional feature space and its temporal behavior, as a complement to existing spatial views. Our approach combines multiple visualizations to assist analysis of time-varying data generated by particle simulations. Coordinated views of both feature and physical spaces allow the observation of particle behavior over specific time periods or the whole temporal domain, rather than describing a single simulation time step. Temporal behavior in the physical space is depicted as *pathlines*, whereas the temporal behavior of the underlying multidimensional feature space is depicted in a so-called *streamfeature visualization*. Streamfeatures are pathlines describing changes in feature space along time, obtained by projecting the feature vectors. Direct interaction with these line representations is difficult. Thus, two supporting views are supplied for user interaction, which show 2D projections of both the pathlines (*pathline projection view*) and the streamfeatures (*streamfeature projection view*), obtained by projecting geometric features extracted from the lines. By linking all visualizations, users may interact with these views to identify and select representative clusters of lines that reflect similar behavior of particle features. We use data from two particle simulations to illustrate the framework and its potential to support analysis of global temporal behavior and relationships between multiple variables.

1 INTRODUCTION

Computer simulations allow the study of phenomena that cannot be observed in real life, e.g., nuclear simulations or simulations of collisions between stars. Particle-based techniques are widely employed in many domains, describing real-world phenomena as systems of discrete particles that have certain properties. Millions of particles may be required to accurately capture system behavior, thus generating very large datasets that are typically time-varying and multi-attribute, as multiple simulation variables describe each particle.

Assisting data analysis in this scenario is challenging, and several high-quality visualization techniques and approaches have been proposed. Most existing solutions focus on representing particles in the physical space, i.e., in the spatial domain of the simulation, at specific time steps. They usually rely on volume rendering solutions, or display particles as glyphs, and temporal behavior is observed from a sequence of such representations. In multivariate simulations, it is likely that users also want to observe the feature (or attribute) space defined by the multiple variables describing particle behavior. A multidimensional feature space may be visualized with techniques such as Parallel Coordinates (Inselberg, 1985), scatterplot matrices or multidimensional projections (Joia et al., 2011; Poco et al., 2011; Paulovich et al., 2010), which have been employed to complement spatial views in multifield volume rendering (Blaas and Post, 2008; Linsen et al., 2008; Linsen et al., 2009; Akiba and Ma, 2007).

In this work we focus on tools for visualizing the feature space in particle simulations, employing multidimensional projections in a framework that allows observing how the underlying feature space evolves. Central to this framework is a line glyph called a *streamfeature*, designed to convey temporal behavior of a particle and reveal meaningful changes in its defining feature space. The streamfeature line is obtained by concatenating particle projections generated for a sequence of simulation time steps. By displaying views of the streamfeatures, we contribute an approach to observe time-varying volumetric datasets derived from multifield particle simula-

S. Reis Santos T., V. Paulovich F., Molchanov V., Linsen L. and C. F. de Oliveira M..
Visualizing Temporal Behavior in Multifield Particle Simulations.
DOI: 10.5220/0004207705730582
In *Proceedings of the International Conference on Computer Graphics Theory and Applications and International Conference on Information Visualization Theory and Applications* (IVAPP-2013), pages 573-582
ISBN: 978-989-8565-46-4

tions in which: (i) particle behavior is observed by coordinating views of both feature and physical spaces (streamfeatures and pathlines, respectively); (ii) similarly to the well-known pathlines in fluid visualization, the streamfeature glyph conveys the global temporal behavior of each particle, as observed in its defining attribute space. Thus, both physical and feature space visualizations embed multiple simulation time steps.

This paper is organized as follows. Section 2 discusses related work on visualizing time-varying data generated by particle simulations. Section 3 provides a short background on multidimensional projection techniques used in this work. The computation of the streamfeature glyph is explained in Section 4. Section 5 describes the framework that incorporates the streamfeature visualization, how it is linked with alternative views and functionalities for data exploration. Section 6 describes usage of the framework to explore data from two particle simulations, and finally Section 7 presents conclusions and further work.

2 RELATED WORK

(Gribble et al., 2006) introduce a GPU-based approach to generate visualizations of very large particle simulation datasets, focusing on generating 3D views on desktop computers at interactive rates. Their solution renders high quality particle glyphs using point sprite rendering and software-based acceleration techniques. It supports several data exploration functions and is fast enough to handle multiple time-varying volumes, but apart from interactivity it offers no specific support for analysis over the temporal domain.

(Falk et al., 2010) also propose an efficient solution for rendering the physical space. They implement a method of sliced ray casting with on-demand volume reconstruction that combines texture slicing, ray casting and splatting. The density field is reconstructed from the particles in screen space at viewport resolution and at the sampling depths used by the volume ray casting. This solution requires less memory than an object-space ray casting and achieves superior image quality and comparable rendering performance.

(Co et al., 2004) are interested in interactive exploratory tools for simulation data in the domain of particle accelerator physics, seeking for solutions capable of depicting views of the feature space. Their suite of tools integrate 2D and 3D scatterplots and a representation of the particles as 3D-shaped glyphs aimed at conveying shape and trends in particle distributions affected by multiple electromagnetic fields. Animation conveys temporal behavior. Authors emphasize that the combination of familiar small multiple scatterplots for rapid multidimensional data exploration with selection and linked views to facilitate visual correlation of similarity results in an effective system for exploratory tasks.

Recent contributions specifically address visualization of time-varying multivariate data and exploit the idea of integrating visualizations of both the physical (object) space and the feature (attribute) space. This is the case of the system by (Jones et al., 2008) to handle time-varying multivariate point-based data from gyrokinetic simulations. The feature space visualization, called *variable visualization*, shows the relationships and trends among the multiple simulation variables and provide an intuitive interface for selecting data items. The object space, or *physical visualization*, shows a spatial representation of the particles as spherical glyphs (with point sprite rendering) at a single time step, and as illuminated pathlines along a range of time steps, with line color and opacity mapping a user selected variable. The variable view is based on an optimized implementation of Parallel Coordinates with brushing and alternative locking modes as enhanced facilities for users to specify selections in multidimensional space. All views are linked, so user selections on the Parallel Coordinates reflect in the physical and other views. The Parallel Coordinates view depicts variable relations at a single time step – for multiple time steps authors use 2D $x-y$ plots of the different variables, with the x-axis representing time.

Our work has many elements in common with that of (Wei et al., 2012), who propose a dual-space visualization approach for studying particle combustion simulation data. By ”dual space” they refer to a combination of the 3D simulation domain in which the particles are advected, referred to as the *physical space*, and the attribute domain, in which the particle attributes evolve, called the *phase space*. The particle's spatial movement in physical space is called its *trajectory*, and its attribute variation in phase space is called its *attribute evolution curve*. The system incorporates user-driven semi-supervised learning to deal with the difficulties of handling and interacting with the large bulk of lines. The attribute evolution curves are clustered using a polynomial regression mixture model, and users can interact with groups to identify and categorize interesting behavior.

We also employ trajectory lines to depict particle behavior in both physical and attribute spaces, inspired by the approach adopted by (Poco et al., 2012) to handle brain fiber tracking data. Authors extract shape features from the 3D lines describing the fibers

in order to generate 2D layouts which separates the lines based on similarity of their global shape. The layout provides an alternative visual interface that facilitates interaction with the fiber lines: by linking both views, bundles of lines with similar behavior may be user selected and further inspected. We generate line icons that summarize particle behavior in attribute space over time, as well as projections of such lines to help users to identify and interact with relevant groups of lines. The same approach is applicable to pathlines that describe particle behavior in physical space.

3 BACKGROUND

Our framework relies on dimension reduction with multidimensional projection. Let X be a set of n data points defined in a d-dimensional space, i.e., $X = \{x_0, x_1, ..., x_n\}$, with $x_i = \{x_{i_1}, x_{i_2}, ..., x_{i_d}\} \in \mathbb{R}^d$. Let Y denote the projection of X in a visual space ($\mathbb{R}^2$ or $\mathbb{R}^3$). $s(\cdot,\cdot)$ is a dissimilarity function criterion between two data points in $\mathbb{R}^d$ and $\hat{s}(\cdot,\cdot)$ is their dissimilarity function criterion defined in the projected space. A multidimensional projection is a technique that obtains Y from X, given $s(\cdot,\cdot)$, usually while attempting to minimize some error measure defined in terms of s and $\hat{s}$.

Many approaches may be applied to project high-dimensional data, e.g., one may obtain visual representations with classical dimension reduction techniques such as Principal Component Analysis (Jolliffe, 2002) or Fastmap (Faloutsos and Lin, 1995) onsidering the 2 or 3 best ranked principal components, or projecting the data points $x_i \in X$ in p mutually orthogonal directions with $p = \{2,3\}$.

The *Force Scheme* (FS) (Tejada et al., 2003) projection adapts the classical Force-Directed Placement (FDP) strategies. It reduces computational cost by considering the pairwise distances between data points, rather than computing forces on a mass-spring model. An initial layout – random or computed with another projection method – is iteratively modified to separate data points projected too close and bring together those placed too far apart, according to an error measure given by the difference between s and $\hat{s}$, i.e., the ideal and the actual pairwise point distances.

Handling time-varying volumes requires techniques capable of handling large datasets and generating temporally coherent projections. The *Part-Linear Multidimensional Projection* (PLMP) (Paulovich et al., 2010) and the *Local Affine Multidimensional Projection* (LAMP) (Joia et al., 2011) are recent solutions that meet such requirements.

The mathematical formulation of PLMP may be seen as a generalization of PCA. A linear transformation mapping to obtain Y from X is inferred from a mapping previously applied to a subset of representative data points. Representatives should be chosen to reflect data density and distribution. According to the authors taking $\sqrt{n}$ random samples is usually a reasonable choice, as the technique is robust to the choice of representatives. PLMP has complexity $O(n)$ and good precision measured by stress values computed for layouts generated for several datasets. Moreover, because its transformation mapping is computed from a reduced subset of points, PLMP is applicable as a streaming projection, as not all data points need to be known *a priori*.

LAMP also relies on selecting and projecting a subset of samples, known as *control points*, from which it builds a family of orthogonal mappings, one for each data point. Users can manipulate the placement of the control points to obtain a satisfactory layout. A reduced number of control points usually suffices to obtain good visual mappings, and albeit slower than PLMP and Fastmap LAMP is also competitive in terms of computational times.

Deciding the best technique to project a dataset is not straightforward, and several quantitative measures help to assess the quality of a layout. They usually attempt to capture to which extent a layout retains the distance distribution observed in the input data space. The well-known Kruskal stress measure (Kruskal, 1964), given by equation (1), attempts to quantify the information loss incurred in the projection mapping.

$$Kruskal = \sqrt{\frac{\sum_{i<j}(\hat{s}(x_i,x_j) - s(x_i,x_j))^2}{\sum_{i<j}\hat{s}(x_i,x_j)}} \quad (1)$$

One may alternatively inspect a scatterplot of the $original\_distances \times projected\_distances$ for all data point pairs, known as *stress curve* (Joia et al., 2011). A hypothetically ideal projection that achieves 100% distance preservation would produce a stress curve with all points plotted along the main diagonal line in the scatterplot.

The *Neighborhood Preservation* (NP) curve (Paulovich et al., 2008), on the other hand, displays the percentage of neighboring points in the input space that remain in the same neighborhood after the projection, for a varying number of neighbors. This value is computed for each data point and averaged over all data points (see Figure 4).

4 GENERATING PARTICLE STREAMFEATURES

A streamfeature is created for a particle by projecting its feature vectors extracted from a temporal sequence of volumes and connecting the projected points into a line. This line describes the particle's temporal evolution, as observed in its defining feature space. Projection may be performed with either PLMP or LAMP, as both have the capability of preserving temporal and spatial coherence when handling time series data. As discussed in Section 3, both techniques require selecting and projecting a representative subset of data points, and the quality of this initial projection affects the quality of the overall result. We thus empirically investigate multiple alternatives, taking the quality measures described in Section 3 as guides to identify the potentially best choice, given a dataset.

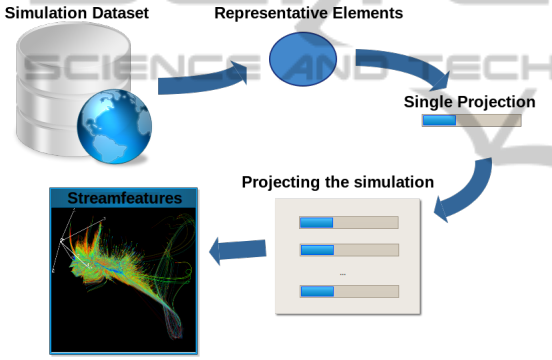

Figure 1: Pipeline of the streamfeature generation process.

Generating streamfeatures comprises three stages, illustrated in Figure 1. Initially, it may be necessary to downsample the volumes for the sequence to fit the primary memory available. This is done by random sampling. The subset of representative data points (required by both PLMP and LAMP) is obtained by taking a random sample from each volume. The representatives' feature vectors must be then projected with a precise technique. Several techniques and distance functions may be considered for this initial projection, and we compare the quality of different layouts to make an informed choice.

We projected the representatives with the classical techniques PCA, Fastmap, Sammon's Mapping and the Force Scheme (Tejada et al., 2003), as well as with recent ones known to be fast and precise, namely LAMP, PLMP and LSP (the *Least Squares Projection*) (Paulovich et al., 2008). Both Sammon's Mapping and Force gradually optimize an initial layout based on an error criterion, so alternative initial layouts may be considered. Overall we investigated 15 projection or dimension reduction techniques and variations – Fastmap, Fastmap with Force Scheme (meaning the former provided an initial layout for the latter), Fastmap with Sammon's mapping, PCA, PCA with Force Scheme, PCA with Sammon's mapping, LAMP, LAMP with Force Scheme, LAMP with Sammon's mapping, PLMP, PLMP with Force Scheme, PLMP with Sammon's mapping, LSP, LSP with Force Scheme, LSP with Sammon's mapping – and distance functions, Euclidean and Mahalanobis, as approximations to dissimilarity $s(\cdot,\cdot)$. Euclidean is a usual choice, and Mahalanobis is known to be effective in normally distributed data with multiple correlated attributes (Tan et al., 2005).

We compare the layouts obtained regarding stress function values, stress curves and neighborhood preservation capability, in order to select the best projection of the representatives for either PLMP or LAMP. In the final stage the remaining particles (the non-representatives) at each time step are projected in 3D, and the projected points relative to a single particle are connected into a line to obtain its streamfeature.

Figures 2 and 3 show box plots of the mean stress values computed for the layouts generated to obtain the streamfeatures for a dataset analyzed in Section 6, considering the Euclidean and the Mahalanobis distances, respectively. The Euclidean layouts with lowest stress are Fastmap with Force Scheme, LAMP with Force Scheme and PCA with Force Scheme; for Mahalanobis are Fastmap, Fastmap with Force Scheme and Fastmap with Sammon's Mapping have the lowest values. Notice that the layouts obtained with Mahalanobis have lower stress values in general.

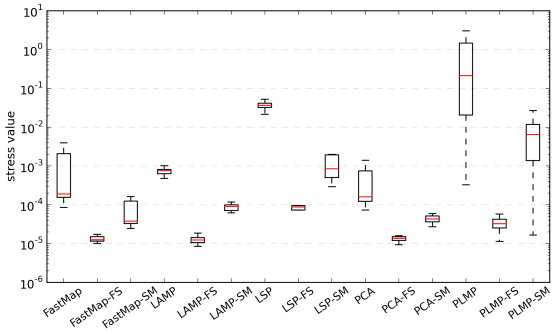

Figure 2: Kruskal stress of 15 layouts computed with distinct techniques and Euclidean distance, for a particular dataset. Best: LAMP-FS, Fastmap-FS and PCA-FS.

The stress curves of the best layouts obtained with both Euclidean and Mahalanobis distances, not shown due to space constraints, indicate that they all do a very good job of preserving original distances, with a slight superiority of the Mahalanobis layouts on this

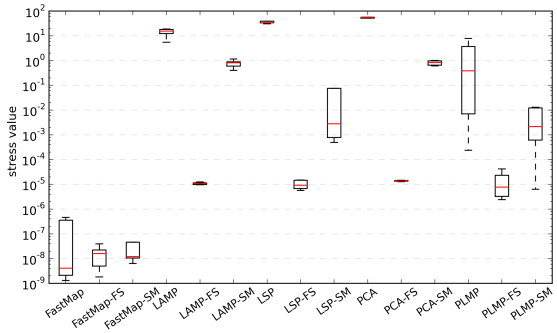

Figure 3: Kruskal stress of 15 layouts (same dataset and techniques) now with the Mahalanobis distance. Best: Fastmap, Fastmap-FS and Fastmap-SM.

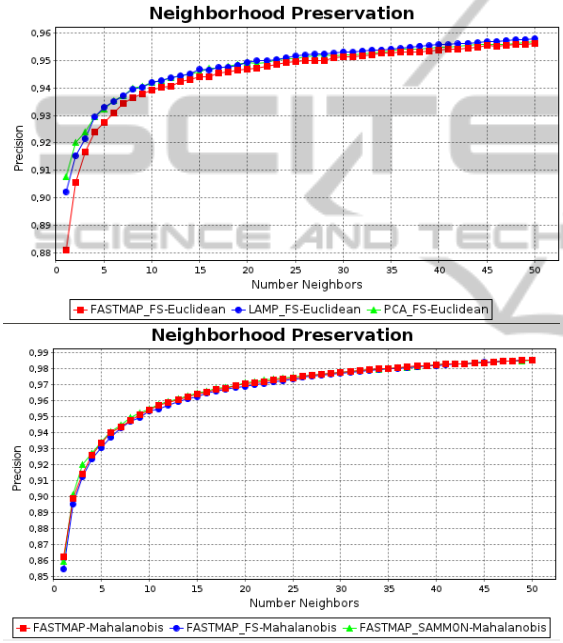

Figure 4: Neighborhood preservation curves of the best layouts (best stress values) computed with Euclidean (top) and Mahalanobis (bottom).

particular dataset.

Figure 4 shows the Neighborhood Preservation curves for the three best (according to stress values) layouts, with the Euclidean (a) and the Malahanobis distances (b). We actually compared the curves for all the layousts, and observed that the techniques with best stress values also display the best behavior regarding neighborhood preservation.

All in all, the layout created with Fastmap with Force Scheme and the Mahalanobis distance attained the best stress and better neighborhood preservation, and is thus a good choice as the initial layout of the representatives in computing the particle streamfeatures for this dataset. A similar comparative analysis should be conducted for any dataset. Streamfeature visualizations generated for different simulations are illustrated in Section 6.

5 VISUALIZATION FRAMEWORK

The framework developed integrates four distinct views to assist interpretation of temporal data. Two of them are the streamfeature and pathline views, both illustrated in Figures 7 and 11, in Section 6, for two distinct simulations. The high density of lines makes it difficult to interact directly with those views, however. We employ multidimensional projections of both the streamfeatures and the pathlines as complementary views to support user interaction, as illustrated in Figure 6. Users may interact with those views to identify and select groups of streamfeatures or pathlines for further inspection, as illustrated in the case studies discussed in Section 6. The projections convey similarity relations over the temporal domain and, as such, help identification of temporal clusters and trends. They also afford interactions such as selection of one or multiple streamfeatures or pathlines. All four views are linked, so that interaction in a projection view, e.g., a selection is reflected in the remaining views.

Projecting the streamfeatures or pathlines requires describing them as multidimensional feature vectors. As our goal is to highlight paths with similar global and local shapes and geometric properties – e.g., starting point, size – so as to reveal similar behavior in feature space, features must be chosen that encode such information. Following the same rationale adopted by (Poco et al., 2012), our feature vectors are formed by low and high frequency coefficients of the Fast Fourier Transform (FFT) of the 3D line (Reddy and Chatterji, 1996), in each principal direction (x, y, z), plus the line's initial and final positions, its size and its center of mass.

The resulting vector is described by 40 attributes: 30 Fourier coefficients (15 low-frequencies in x, y and z; 15 high-frequencies in x, y and z,) plus 10 geometrical coefficients, namely the (x, y, z) coordinates of the starting point, idem for the final point and the center of mass point, plus the line size. This choice places a dominance of shape attributes (Fourier coefficients) over the geometric ones. A more balanced distribution of shape and geometric attributes may be desirable depending on the goals, e.g., if the goal is to favour perception of similar line shapes in nearby regions. It is thus possible to vary the weights assigned to the features prior to projection. In the examples discussed in Section 6 the line features were projected

with LAMP.

Users may select individual elements or groups in the projection views, and track the selection in the pathline and streamfeature views. They can manually identify groups of particles with similar behavior by delimiting visual clusters in the projection, or alternatively an X-means clustering (Pelleg and Moore, 2000) may be applied to identify clusters automatically. This is an extension of k-means clustering that finds the optimal number of clusters that best models the data, within a given range. Once obtained, clusters are color coded in the projection, as illustrated in Figure 6. Users may select one or multiple clusters and inspect their behavior in the pathline or streamfeature feature projection views. The ability to interact with groups is particularly useful, as the original line views are typically very cluttered. Users may also choose to observe behavior over a time range, rather than over the whole simulation time.

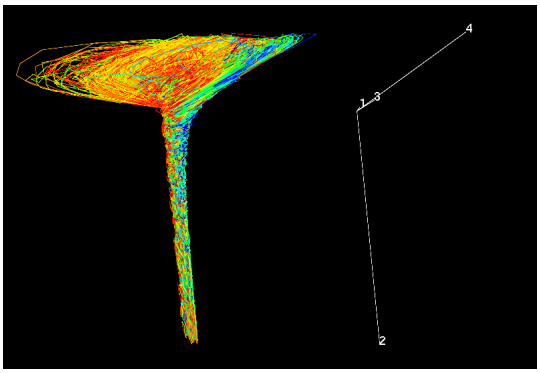

Figure 5: Streamfeatures for the whole simulation and axes in 9-dimensional attribute space (Exploding Stars).

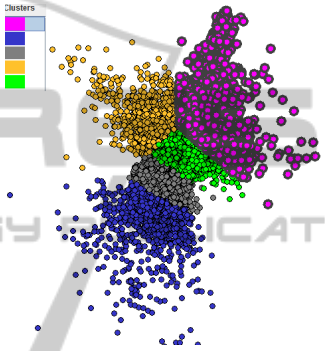

Figure 6: X-means clusters in the projection view. The pink cluster has been selected and its elements are shown highlighted (thicker borders).

6 EXPLORING SIMULATION DATA

We illustrate the techniques on data derived from Smoothed Particle Hydrodynamics (SPH) simulations (Linsen et al., 2011) and made available by collaborators, identified as the **Merging Stars** and the **Exploding Stars** datasets. Both datasets represent binary star systems consisted of two White Dwarfs each. Simulations include thousands of time steps, of which only a small part is used for analysis and visualization. Several scalar and vector fields are recorded, including physical quantities (velocity, gravity, mass, etc.), chemical fractions and computational parameters (radius of influence of particle, artificial viscosity coefficient and others).

6.1 Merging Stars

In this simulation one of the modeled objects (the donor star) is being destroyed when its mass gradually flows to the second star (accretor) under strong gravitational force. Two White Dwarfs are discretized by means of 2.5M particles carrying the following scalar quantities: radius of influence, density, temperature, and artificial viscosity.

As discussed in Section 4, the streamfeatures view for these data have been created using Fastmap with Force Scheme to project the representatives, LAMP and the Mahalanobis distance. The streamfeatures view relative to the whole simulation is shown in Figure 5. The multidimensional axes describing the streamfeature space are shown displaced. In this and in the following figures that adopt the rainbow scale, color mapping indicates time evolution: blue corresponds to initial stages of the simulation, and red indicates final stages. The Cartesian axes in the four-dimensional attribute space have undergone the same projection transformation applied to the data, and provide a visual hint of the attributes undergoing dominant changes in the temporal domain and the direction of change – from the figure one observes that attributes *density* (axis 2) and *artificial viscosity* (axis 4) are dominant in the temporal domain.

The streamfeatures and pathlines were projected with LAMP using the Mahalanobis distance, but the resulting layouts are very dense and cluttered, hampering perception of groups of similar elements. The result of applying an X-means clustering to both projections can be seen in Figure 6, which depicts the 5 clusters identified – we input a range $[5,50]$ for the number of clusters to be sought for by X-means. We computed the silhouette coefficients of the resulting clusterings. This is a measure of cluster quality (Tan et al., 2005) that takes values in the range $[-1.0,1.0]$, where values closer to 1.0 indicate well separated and highly cohesive groups. Silhouette values of 0.416 and 0.799 were obtained for the pathline

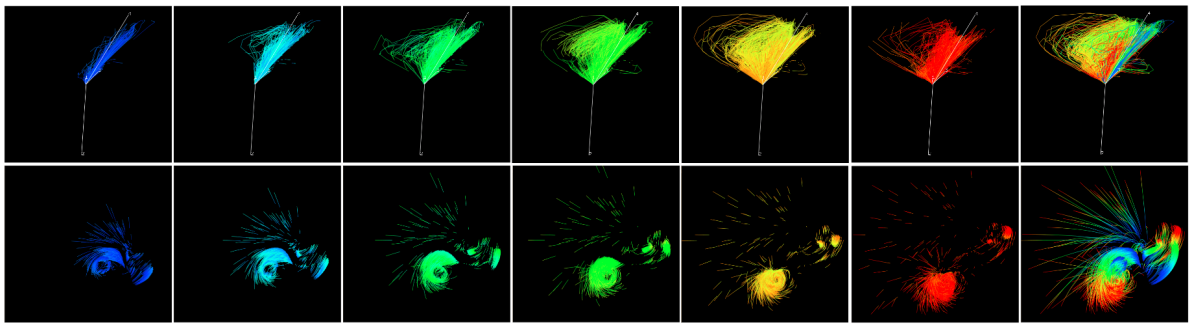

Figure 7: Merging Stars simulation: top row images show the streamfeatures describing the behavior of a selected cluster of particles, bottom row images show the corresponding pathlines. The rightmost images cover the whole simulation (59 time steps), whereas the previous ones show streamfeatures and pathlines computed over a sequence of size 10 time windows, namely 0-10, 10-20, 20-30, 30-40, 40-50 and 50-59. Most particles are moving towards the center of the two stars, and one observes little variation occurring in the direction of attribute *density* (axis 2, the long vertical line in the central region).

and the streamfeature clusters, respectively. The second value indicates well-formed clusters that group similar-shaped streamfeature lines, as measured by the Mahalanobis distance. Thus, they likely depict similar particle trajectories in feature space.

Figure 7 shows evolution of the particles in the pink cluster selected in Figure 6, with blue to red mapping time evolution. This particular cluster has 2,007 particles, or 1.61% of the total particles tracked. The top row shows images of the streamfeatures and the bottom row shows the corresponding pathlines, computed over different simulation time periods. Interpreting a visualization that covers the whole temporal domain is not straightforward, it may thus be interesting to observe behavior over shorter time intervals, e.g., as shown in the figure, over windows of size 10, corresponding to 10 simulation time steps.

The pathlines in Figure 7 indicate that particles in this group are being attracted to the center of the two stars. In the streamfeature views we notice that major changes occur in the directions associated to attributes *radius* (axis 1), *temperature* (axis 3) and *artificial viscosity* (axis 4), while no major changes are observed in the direction associated to attribute *density* (axis 2) for this particular cluster. Furthermore, notice that changes were initially localized around the direction defined by attribute *artificial viscosity* (4), but then from time interval 40-50 the attributes *radius* (1) and *temperature* (3) start playing a more dominant role in particle behavior. Figure 8 shows rotated views of the rightmost images in Figure 7, illustrating possible user interactions with these 3D representations.

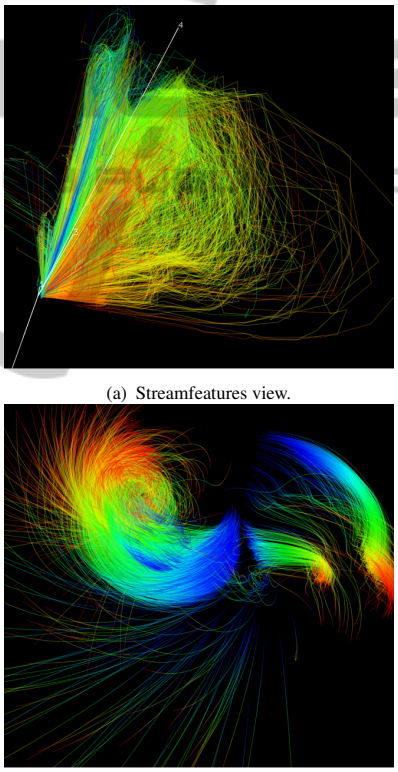

(a) Streamfeatures view.

(b) Pathlines view.

Figure 8: Rotated views of the visualizations in the last column of Figure 7 (Merging Stars).

6.2 Exploding Stars

In the second simulation, extremely high temperatures are reached during stars interactions. This serves as an indicator for the start of nuclear burning that later will – although this phase has not been simulated and is not presented in the data – lead to the explosion of stars. This simulation tracks 39,200 particules and the number of attributes is 13, of which 9 were chosen for analysis. They are: radius of influence, internal energy, temperature, several chemical components, and the mean number of nucleons per isotope (“abar”).

The streamfeatures have been generated employ-

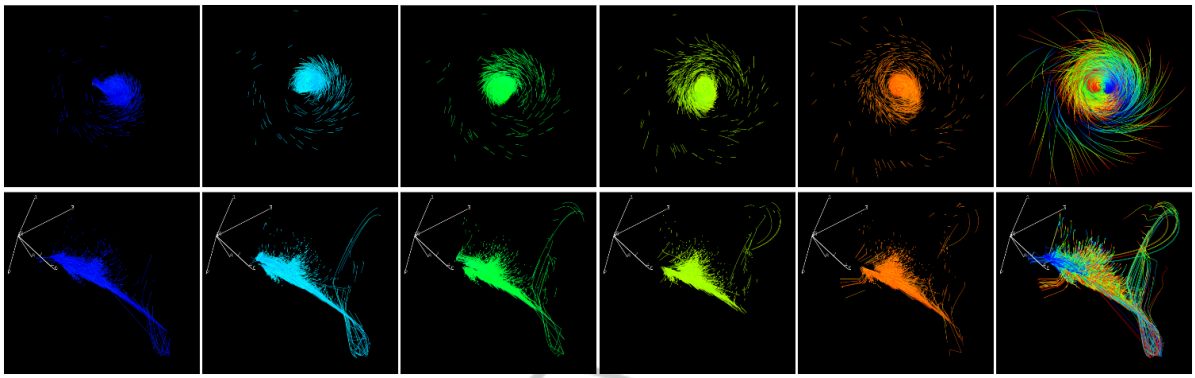

Figure 11: Pathlines (top) and streamfeatures (bottom) of a selected cluster in the Exploding Stars simulation. The rightmost images display the streamfeatures and pathlines computed over the whole simulation (200 time steps). Left to right: a sequence of streamfeatures and pathlines for time windows of size 20, namely 0-20, 40-60, 80-100, 120-140 and 160-180.

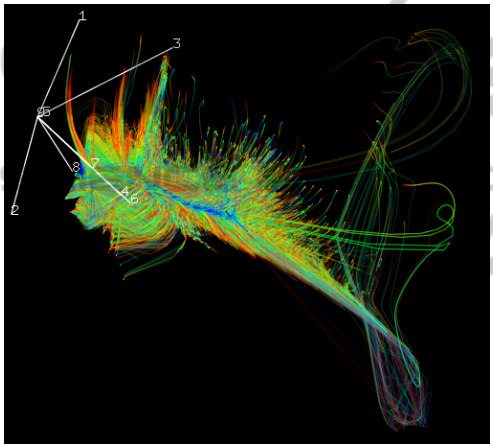

Figure 9: Streamfeatures for the whole simulation, shown with axes in 9-dimensional attribute space (Exploding Stars).

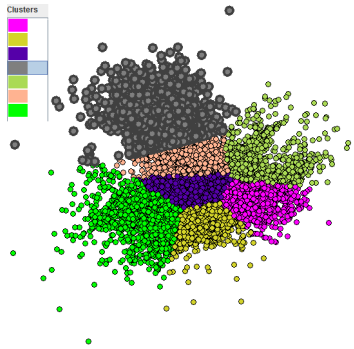

Figure 10: X-means clusters in the streamfeature feature projection, with a cluster selected and highlighted.

ing Fastmap with Force Scheme, LAMP and the Mahalanobis distances as the dissimilarity functions, after considering several alternatives and conducting an analysis similar to that detailed for the Merging Stars data. The resulting streamfeatures for the whole simulation are shown in Figure 9.

The projection of the features extracted from the streamfeatures, computed with LAMP and Mahalanobis, appears in Figure 10, with clusters color coded. X-Means identified 7 clusters as the best configuration (searching in the range $[5,50]$). The compued silhouette coefficient is 0.482, indicating clusters not as well-formed as in the previous example.

Figure 11 shows the evolution of the cluster selected in Figure 10, which includes 6,883 particles, 17.56% of the total. Images in the top row depict the particle pathlines and in the bottom row the corresponding streamfeatures are shown. One notices that some particles in this group are trapped in the gravitational field of the star, those seen in the central circular shape in the pathline views, whereas others seem to escape the star attraction and are lost to space, shown by the pathlines tangent to the circular shape. As the simulation starts the major directions of change seem to be associated with attributes *Helium*, *Neon* and *Magnesium* (axes 4, 6 and 7, respectively), attributes *radius* and *temperature* apparently start playing a major role as it evolves (notice the outgoing lines at the right region of the streamfeature views).

An interface widget is provided for users to filter the pathlines to be displayed according to their size, by setting lower and upper size thresholds. This allows them to focus, e.g., on analyzing a subset of particles with greater (or smaller) displacement in the object space. Visualizations after such filtering are illustrated in Figure 12: they cover the whole simulation, but shown are only lines that survived the filtering. Each column shows a view of the pathlines (top) and the corresponding streamfeatures (bottom).

From left to right, images in the first column display the object and feature space behavior of 3 particles, then 12, 441 and 1,880 particles, respectively: the first three views show only particles with high displacement, whereas the last one shows particles with

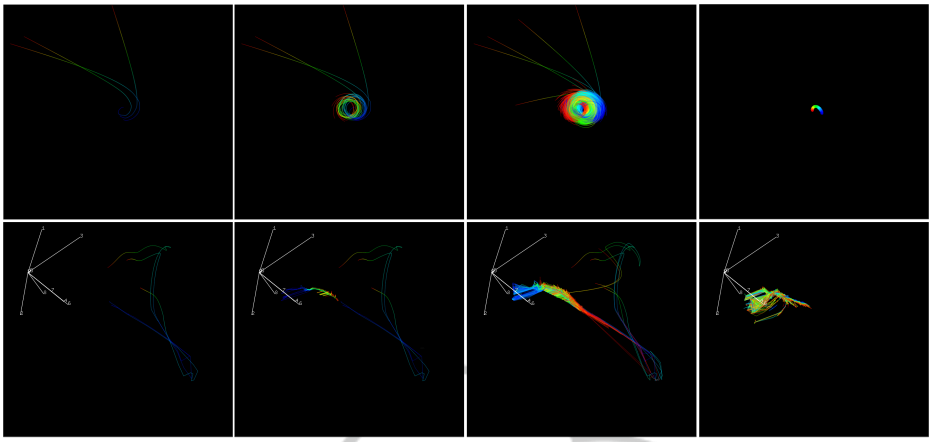

Figure 12: A view of the pathlines (top) and streamfeatures (bottom) filtered by their size. From left to right, images display the object and feature space behaviors of 3, 12, 441 and 1,880 particles, respectively, along the Exploding Stars simulation.

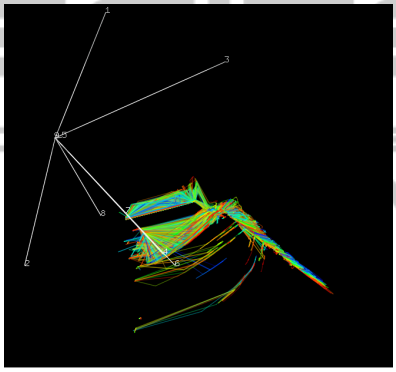

(a) Streamfeatures.

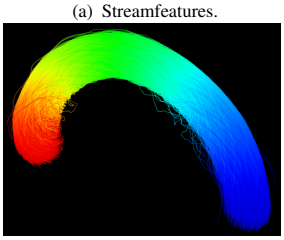

(b) Pathlines.

Figure 13: Observing behavior of 1,880 particles filtered based on their spatial displacement: particles with small displacement.

low displacement. One observes that most particles show reduced spatial displacement, highly concentrated in the central region, whereas the three particles with higher displacement wander away from this central area.

Behavior of the 1,880 particles with small spatial displacement in the simulation is better observed in the views in Figure 13. Figure 14 shows projected views of the features extracted from the pathlines and the streamfeatures, highlighting the particles filtered.

(a) Pathline projection. (b) Streamfeature projection.

Figure 14: Projections of the streamfeature and pathline features: 1,880 low-displacement particles highlighted.

7 CONCLUSIONS

We developed a framework to support the exploratory visualization of data generated by multifield particle simulations. This is a challenging problem that requires handling a temporal sequence of multi-attribute volumes and assessing and interpreting time-varying multidimensional information. Our framework integrates visualizations of both the spatial (physical) and the feature space domains, and includes functionalities for users to observe and interpret particle temporal behavior in both spaces simultaneously. This is achieved by combining multiple coordinated views of both feature and physical spaces to allow the observation of particle behavior over the whole temporal domain or over selected time windows, rather than restricting users to handling a single simulation time step.

The feature space visualization relies on an analog of the well-known pathlines for visualizing fluid behavior. This view suffers with overcrowding as the number of particles increases, quickly aggravated when handling simulations over many time steps. This is handled with clustering and filtering functionalities and with projected representations of feature

vectors extracted from the lines. Usage of the framework has been illustrated on data from two SPH simulations in astrophysics. We intend to investigate further the feature extraction procedures adopted to generate the projection views of pathlines and streamfeatures, as other alternatives might produce different outcomes. Distortion errors are likely introduced in the projection processes, and how they affect exploration of temporal behavior also deserves a careful investigation, in line with validation of the framework in cooperation with domain experts.

ACKNOWLEDGEMENTS

Authors acknowledge the financial support of FAPESP, CNPq, CAPES-DAAD-PROBRAL, DFG under contract number LI 1530/6-2 and are grateful to S. Rosswog and M. Dan, from Jacobs University, Bremen, Germany, for the simulation datasets.

REFERENCES

Akiba, H. and Ma, K.-L. (2007). A tri-space visualization interface for analyzing time-varying multivariate volume data. In *Proc. Eurographics/IEEE VGTC Symp. Visualization*, pages 115–122.

Blaas, J. and Post, C. P. B. F. (2008). Extensions of parallel coordinates for interactive exploration of large multi-timepoint data sets. *IEEE Trans. Vis. Computer Graphics*, 14(6):1436–1451.

Co, C. S., Friedman, A., Grote, D. P., Vay, J.-L., Bethel, Wes, E., and Joy, K. I. (2004). Interactive methods for exploring particle simulation data. Lawrence Berkeley National Laboratory.

Falk, M., Grottel, S., and Ertl, T. (2010). Interactive image-space volume visualization for dynamic particle simulations. In *SIGRAD*.

Faloutsos, C. and Lin, K.-I. (1995). FastMap. In *Proc. ACM SIGMOD Int. Conf. Management of Data*, pages 163–174, New York, New York, USA. ACM Press.

Gribble, C. P., Stephens, A. J., Guilkey, J. E., and Parker, S. G. (2006). Visualizing particle-based simulation datasets on the desktop. In *British HCI Works. on Combining Visualization and Interaction to Facilitate Scientific Exploration and Discovery*, pages 111–118.

Inselberg, A. (1985). The plane with parallel coordinates. *The Visual Computer*, 1(2):69–91.

Joia, P., Paulovich, F. V., Coimbra, D., Cuminato, J. A., and Nonato, L. G. (2011). Local affine multidimensional projection. *IEEE Trans. Vis. Computer Graphics*, 17(12):2563–71.

Jolliffe, I. T. (2002). *Principal Component Analysis*. Springer.

Jones, C., Ma, K.-L., Ethier, S., and Lee, W.-L. (2008). An integrated exploration approach to visualizing multivariate particle data. *Computing in Science and Engineering*, 10(4):20–29.

Kruskal, J. B. (1964). Multidimensional scaling by optimizing goodness of fit to a nonmetric hypothesis. *Psychometrika*, 29(1):1–27.

Linsen, L., Long, T. V., and Rosenthal, P. (2009). Linking multi-dimensional feature space cluster visualization to surface extraction from multi-field volume data. *IEEE Comp. Graph. and Applications*, 29(3):85–89.

Linsen, L., Molchanov, V., Dobrev, P., Rosswog, S., Rosenthal, P., and Long, T. V. (2011). *Hydrodynamics - Optimizing Methods and Tools*, chapter SmoothViz: Visualization of Smoothed Particles Hydrodynamics Data. inTech.

Linsen, L., Van Long, T., Rosenthal, P., and Rosswog, S. (2008). Surface extraction from multi-field particle volume data using multi-dimensional cluster visualization. *IEEE Trans. Vis. Computer Graphics*, 14(6):1483–90.

Paulovich, F. V., Nonato, L. G., Minghim, R., and Levkowitz, H. (2008). Least square projection: a fast high-precision multidimensional projection technique and its application to document mapping. *IEEE Trans. Vis. Computer Graphics*, 14(3):564–75.

Paulovich, F. V., Silva, C. T., and Nonato, L. G. (2010). Two-phase mapping for projecting massive data sets. *IEEE Trans. Vis. Computer Graphics*, 16(6):1281–90.

Pelleg, D. and Moore, A. (2000). X-means: Extending k-means with efficient estimation of the number of clusters. In *Proc. 7th. Int. Conf. Machine Learning*, pages 727–734. San Francisco.

Poco, J., Eler, D., Paulovich, F., and Minghim, R. (2012). Employing 2d projections for fast visual exploration of large fiber tracking. *Comput. Graph. Forum*, 31(3):1075–1084.

Poco, J., Etemadpour, R., Paulovich, F., Long, T., Rosenthal, P., Oliveira, M., Linsen, L., and Minghim, R. (2011). A framework for exploring multidimensional data with 3D projections. *Comput. Graph. Forum*, 30(3):1111–1120.

Reddy, B. S. and Chatterji, B. N. (1996). An FFT-based technique for translation, rotation, and scale-invariant image registration. *IEEE Trans. Image Processing*, 5(8):1266–71.

Tan, P.-n., Steinbach, M., and Kumar, V. (2005). *Introduction to Data Mining*. Addison Wesley, Boston, MA.

Tejada, E., Minghim, R., and Gustavo Nonato, L. (2003). On improved projection techniques to support visual exploration of multi-dimensional data sets. *Information Visualization*, 2(4):218–231.

Wei, J., Yu, H., Grout, R., Chen, J., and Ma, K.-L. (2012). Visual analysis of particle behaviors to understand combustion simulations. *IEEE Comput. Graph. Appl.*, 32(1):22–33.